Nonmonotonic Constitutive Laws and the Formation of Shear-Banded Flows

N. Spenley, X. Yuan, M. Cates

Nonmonotonic Constitutive Laws and the Formation of Shear-Banded Flows

N.A. Spenley ([1,2,*]), X.F. Yuan ([1,3]) and M.E. Cates ([1,4])

([1])Cavendish Laboratory, Madingley Road, Cambridge CB3 0HE, U.K.
([2])Max-Planck-Institut für Kolloid- und Grenzflächenforschung, Kantstrasse 55, 14513 Teltow, Germany
([3])H. H. Wills Physics Laboratory, University of Bristol, Royal Fort, Tyndall Avenue, Bristol BS8 1TL, U.K.
([4])Department of Physics, University of Edinburgh, King's Buildings, Mayfield Road, Edinburgh EH9 3JZ, U.K.

(Received 18 September 1995, received in final form 29 November 1995, accepted 3 January 1996)

PACS.47.50.+d – Non-Newtonian fluid flows
PACS.83.10.Ji – Fluid dynamics (non-linear fluid)
PACS.83.20.Hn – Structural and phase changes

Abstract. — We consider constitutive models of viscoelastic behaviour which predict a shear stress which is a nonmonotonic function of the shear rate. It is known that a homogeneous shear flow is unstable when the shear stress decreases with shear rate. We use a novel simulation technique (the Lagrangian-Eulerian method for the fluid dynamics combined with Öttinger's stochastic method for the constitutive equation) to solve one- and two-dimensional models of plane Couette flow for an integral constitutive equation describing entangled wormlike micelles. The results are compared with those of a 'toy' model (with a differential constitutive equation). We show that the steady state actually consists of bands of different shear rate. Such a flow is strongly inhomogeneous, and our preliminary results indicate that the constitutive equation must be modified to allow for spatial variations in the viscoelastic stress.

1. Introduction

Several important models of viscoelastic behaviour, in polymers and other materials, predict that the steady shear stress decreases with shear rate κ, when κ is large enough. For instance, Doi and Edwards' theory [1] shows this behaviour; in their model, at high shear rate, the polymers become aligned along the flow direction, and can no longer generate a shear stress. Some phenomenological models have this property too, such as the corotational Maxwell (CRM) model [2]. On physical grounds, we do not expect this behaviour to persist to indefinitely high shear rate. For example, if a Newtonian solvent is present, the Newtonian viscosity might eventually dominate. Alternatively, the models may fail, as short relaxation-time processes in the polymer itself become important [3], causing the stress to increase. However, these effects are comparatively weak, so that there may still be a range of shear rates where the shear

(*) Author for correspondence (e-mail: spenley@mpikg-teltow.mpg.de)

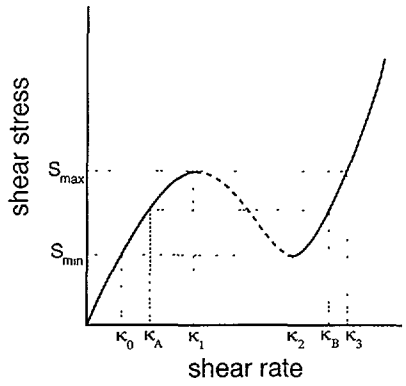

Fig. 1. — Schematic nonmonotonic steady shear stress/shear rate curve

stress is decreasing, Figure 1. This is significant, because a steady flow is unstable under these conditions [4].

Is this behaviour shown by real materials? The most important experimental indication comes from the 'spurt effect', which is shown by many linear polymers in pipe flow. On increasing the driving pressure gradient P' beyond a critical value, the volume throughput is seen to increase discontinuously. When P' is reduced, the throughput decreases gradually, showing hysteresis. For reviews, see [5,6].

This behaviour has been explained in terms of a nonmonotonic shear stress [7–9]. The spurt effect seems to be a transition from a classical Poiseuille-like flow, to a 'plug' flow, in which a gently sheared central cylinder (the plug) is surrounded by an outer layer of strongly sheared material. An alternative explanation, in terms of wall slip, is possible, but in this paper we will assume that the no-slip boundary condition is valid.

Rheometrical experiments are often done in cone-and-plate or cylindrical Couette apparatus. In these geometries, one expects the flow to have the same shear rate everywhere, but this is impossible if the applied shear rate κ_{applied} lies in the region of decreasing stress [4]. What is the analogy of plug flow here, or is a stable, steady flow possible at all? Cates, McLeish and Marrucci (CMM) [10] noted that, in simple shear, the shear stress is a constant throughout the material, so that two shear rates, κ_A and κ_B, can coexist if they correspond to the same steady shear stress: $S(\kappa_A) = S(\kappa_B)$. They suggested that the flow takes a banded form, containing regions with shear rate κ_A, and regions with κ_B, with volume fractions x_A and x_B such that their *average* shear rate equals whatever rate is applied: $\kappa_{\text{applied}} = x_A\kappa_A + x_B\kappa_B$ (with $x_A + x_B = 1$). If κ_{applied} lies between κ_0 and κ_3 (see Fig. 1), then a banded flow is possible (although a uniform flow is forbidden only if κ_{applied} lies between κ_1 and κ_2).

If a banded flow is present, the shear stress is not determined by κ_{applied}, but can lie between $S_{\min}$ and $S_{\max}$. CMM argued that the stress is determined by the flow history, and that if κ_{applied} is increased from zero, the entire flow remains on the low-shear stable branch of the curve for as long as possible. Then, when κ_1 is reached, a small amount of material begins to shear at κ_3 ('top-jumping'). As κ_{applied} is increased further, the proportion of κ_3 increases, until the whole of the sample is being sheared at this rate. The flow is now uniform again, and remains so if κ_{applied} is increased still more. In short, it is assumed that $\kappa_A = \kappa_1$ and $\kappa_B = \kappa_3$. The hallmark of this behaviour is that, in the shear-banded regime, the shear stress is independent of κ_{applied} (and equals $S_{\max}$). Once the flow is in the uniform high shear rate regime, then, on decreasing κ_{applied}, the homogeneous shear flow may persist until κ_2 is reached,

and only then are the shear bands reformed ('bottom-jumping'). In this case, we would expect to observe hysteresis in the stress.

Such behaviour appears not to have been observed for ordinary polymers. Typically, some shear-thinning occurs at higher shear rates, but the shear stress continues to rise gently. However, a surfactant solution (cetylpyridinium chloride and sodium salicylate in water) shows the constant stress plateau predicted by CMM [11]. This surfactant forms highly elongated wormlike micelles, which can entangle, and appear to share many of the rheological features of polymers (for a review, see [12]). Cates has formulated a constitutive equation [13] for them, based on that of Doi and Edwards. Using this equation, together with the shear-banding ideas of reference [10], Spenley, Cates and McLeish were able to predict, with good accuracy, the observed shear stress in the cetylpyridinium system [14]. Direct evidence for shear-banding (birefringence experiments) has recently been found [15] in another entangled micellar system (aqueous cetyltrimethylammonium chloride). Shear-banding has also been reported in references [16,17], although here the behaviour is complicated by the fact that the high-shear band is a shear-induced (metastable) nematic phase [18–20].

The aim of this paper is to test theoretically the shear-banding conjecture, by modelling the start-up of shear flow in a viscometric experiment. In Section 2, we set up the mathematical model, and in Section 3 we try to predict some of its properties. Section 4 analyses linear perturbations on a uniform shear flow. Preliminary numerical calculations are presented in Section 5 for a one-dimensional, and in Section 6 for a two-dimensional model. In Section 7, a modification of the constitutive model is suggested to describe the interface between bands more accurately.

2. Mathematical Formulation

The problem can be modelled at several levels of sophistication. A 3-dimensional model would include the whole experimental geometry (e.g. cone-and-plate), with free fluid surfaces if appropriate. A '(2+1)-dimensional' model would be essentially the same, except that axial symmetry is assumed, so the stress and velocity fields are functions of two variables only. The 2-dimensional model is planar Couette (extending to infinity, so there are no free surfaces). The '(1+1)-dimensional' model is the same as the 2-dimensional, except that symmetry along the shear direction is assumed (so the fields are functions of one variable). For simplicity, we will consider only the (1+1)-dimensional and 2-dimensional models.

We begin with the generalised Navier-Stokes equation for a viscoelastic material in a Newtonian solvent (or with some very short relaxation time modes that can adequately be modelled as Newtonian)

$$\rho\left(\frac{\partial \mathbf{v}}{\partial t}+\mathbf{v}\cdot\nabla\mathbf{v}\right)=\nabla\cdot(\boldsymbol{\sigma}+\eta\nabla\mathbf{v}-p\mathbf{1})\,, \tag{1}$$

where $\mathbf{v}(\mathbf{r})$ is the velocity field, $\boldsymbol{\sigma}(\mathbf{r})$ is the viscoelastic part of the stress, p is the hydrostatic pressure, η is the viscosity of the solvent and ρ is its density. Later, we will have to specify a constitutive equation, but at first we will consider a completely general constitutive behaviour.

We have two rheometer plates parallel to the x-axis, separated by distance L. We distinguish two cases. If the stress is the control parameter, then the boundary condition is that the total shear stress $S=\sigma_{xy}+\eta\partial v_x/\partial y$ is fixed, thus

$$\sigma_{xy}+\eta\partial v_x/\partial y=S_{\text{applied}} \quad \text{for } y=0,L. \tag{2}$$

On the other hand, if the shear rate is the control parameter, then the boundary condition is on the velocity

$$\mathbf{v}(x, y = 0, z) = \mathbf{0} \quad (3)$$

$$\mathbf{v}(x, y = L, z) = U\hat{\mathbf{x}}. \quad (4)$$

This gives an average shear rate of $\kappa = U/L$.

The (1+1)-dimensional condition is that $\mathbf{v}(\mathbf{r}) = v(y)\hat{\mathbf{x}}$ (so that all the streamlines are straight and parallel, the flow everywhere is in the x-direction, and the velocity can change across the flow, but not along it). Equation (1) reduces to

$$\rho\frac{\partial v}{\partial t} = \frac{\partial}{\partial y}\left(\sigma_{xy} + \eta\frac{\partial v}{\partial y}\right). \quad (5)$$

The normal stresses have been eliminated and play no role in the dynamics, nor can we obtain any information about the normal force exerted on the plates. In a real experiment, this can be measured by the rheometer and used to calculate the first normal stress difference.

A very similar problem to pipe flow, that of flow down a slit channel, was studied by Malkus, Pego and others at the University of Wisconsin [9,21–23]. They used a (1+1)-dimensional approach, with an equation identical to equation (5) apart from a driving pressure term (and different boundary conditions). Their constitutive relation was the corotational Maxwell equation (in fact, they began with the Johnson-Segalman model [24] with a single relaxation time, but were able to show that, for their problem, this can be replaced by the CRM equation without loss of generality). They found that the final steady state is a plug flow.

In a two-component system, such as an aqueous solution of micelles, there may be some coupling between the mechanical properties and the local composition. This is discussed in reference [25]. We neglect this effect in the present work. In any case, it does not arise in a one-component system such a polymer melt.

3. A Toy Constitutive Model

We introduce a simple constitutive model to help elucidate the behaviour of equation (5)

$$\frac{\partial\sigma}{\partial t} + \frac{\sigma}{\tau} = Gg\left(\tau\frac{\partial v}{\partial y}\right). \quad (6)$$

This is the simplest possible constitutive equation that can show both viscoelasticity (i.e. a finite relaxation time) and nonlinear response. Here σ is the viscoelastic shear stress (denoted σ_{xy} in the previous section, but we drop the subscript here for simplicity), while τ is the viscoelastic relaxation time and G is the elastic modulus. The function g is the viscoelastic shear stress as a function of the shear rate in steady shear flow, and may be chosen freely. This toy model is deficient in that it is not written in tensor form, but for the purposes of (1+1)-dimensional modelling, this is irrelevant.

Equation (6) has already been studied in the context of slit flow [23]. Following reference [23], we will use this form for g:

$$g(\xi) = \frac{\xi}{1 + \xi^2}. \quad (7)$$

The total stress $S = \sigma + \eta\partial v/\partial y$ is then nonmonotonic, provided $\eta/G\tau < 1/8$, which we will always assume to be true.

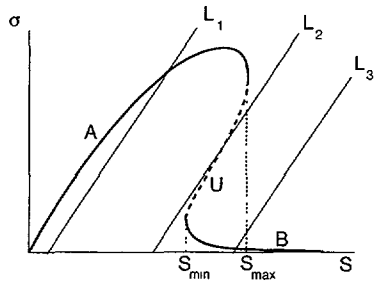

Fig. 2. — Schematic phase diagram for the viscoelastic stress σ, with the total stress S as the control parameter. The solid and dashed lines indicate stable and unstable equilibria respectively. L_1, L_2 and L_3 are lines of constant shear rate.

We begin with the stress-controlled regime. Assuming creeping flow (i.e. the fluid density $\rho = 0$), equations (2) and (5) give

$$\sigma + \eta \frac{\partial v}{\partial y} = S_{\text{applied}}. \tag{8}$$

This allows us to eliminate $\partial v/\partial y$ from equation (6), leaving an equation in the single variable σ, with S_{applied} as a parameter. Notice that the spatial derivative $\partial/\partial y$ has disappeared. This means that the stresses at different positions evolve independently, or (in other words) that the streamlines have been decoupled from one another. The behaviour of the system is now trivial. Equation (6) may be written in the form

$$\frac{\partial \sigma}{\partial t} = -\frac{1}{\tau} \frac{\partial V(\sigma)}{\partial \sigma} \tag{9}$$

where $V(\sigma)$ is

$$V(\sigma) = \frac{1}{2}\sigma^2 + \frac{G\eta}{2} \ln\left(1 + \frac{1}{\eta^2}(S - \sigma)^2\right). \tag{10}$$

V has two minima if $S_{\min} < S_{\text{applied}} < S_{\max}$ (and $\eta/G\tau < 1/8$), otherwise it has one. It follows that for $S_{\text{applied}} < S_{\min}$ and $S_{\text{applied}} > S_{\max}$, σ has one equilibrium point. For $S_{\min} < S_{\text{applied}} < S_{\max}$, there are two stable equilibria and one unstable. This is summarised in Figure 2. Branch A corresponds to low shear rates, where most of the stress is due to the viscoelastic material, and branch B to high shear rates, where the polymer (or whatever the material is) has been strongly aligned and can no longer generate a stress, so most of the stress is Newtonian.

We are dealing with a macroscopic system, and σ is in principle a function of the y-coordinate (in the (1+1)-dimensional approximation). Normally, σ would be constant with respect to position in the stress-controlled regime, but this is not necessarily the case. It is possible for different parts of the flow — different streamlines — to be on different stable branches of the phase diagram, Figure 2. By a suitable control of S_{applied}, the system may be taken to a point on the unstable branch. Fluctuations will then carry some streamlines into one of the basins of attraction, and the rest into the other, and subsequent evolution will yield a 'banded' flow.

We now take the shear rate as the control parameter. Again with creeping flow, equation (5) becomes

$$0 = \frac{\partial}{\partial y}\left(\sigma + \eta \frac{\partial v}{\partial y}\right). \tag{11}$$

The total shear stress $S = \sigma + \eta\partial v/\partial y$ is therefore again constant in space. Using the boundary conditions (3)–(4),

$$\sigma(y) + \eta\frac{\partial v(y)}{\partial y} = \langle\sigma\rangle + \eta\kappa, \tag{12}$$

where $\langle\sigma\rangle$ is defined to be $(1/L)\int_0^L \sigma(y)\mathrm{d}y$. Again, this equation may be used to eliminate $\partial v(y)/\partial y$, but now the streamlines are not quite independent; they are coupled to one another via the average value of the viscoelastic stress $\langle\sigma\rangle$. The total shear stress S now varies with time. As long as the flow remains homogeneous, so that σ at every point is equal to $\langle\sigma\rangle$, the state of the system is represented by a point on the line $S = \sigma + \eta\kappa$. In Figure 2, L_1, L_2 and L_3 are such lines for, respectively, $\kappa < \kappa_1$, $\kappa_1 < \kappa < \kappa_2$ and $\kappa > \kappa_2$. If the applied shear rate is on one of the stable branches, then the system evolves in time, always remaining on the line (L_1 or L_3), and moving along it until it reaches the equilibrium manifold and attains a final stable (homogeneous) state. If the applied shear rate is in the unstable regime, then the system cannot simply evolve along the line L_2. Instead, the fluctuations grow, and the streamlines diverge from each other and from L_2. (A more precise discussion of this is given in the next section.) A steady state is now reached only when every streamline is on one or other of the two stable branches A or B, so that the flow is banded.

Couette-like flow with controlled stress is closely related to flow through a pipe. The difference is that each point on the radius of the pipe has a different stress (determined by the driving pressure gradient), whereas in Couette flow, the stress is constant throughout the flow. Since, in creeping flow, the streamlines may be decoupled, this is not of fundamental importance. In Couette geometry, the flow will normally be homogeneous (unless the applied stress is deliberately manipulated in a very careful way), and in the pipe, the flow will be either Poiseuille-like or take a simple plug form.

By contrast, in the shear-rate controlled regime, the streamlines can never be fully decoupled, and the distribution of σ across the streamlines must be explicitly taken into account. With a banded flow, the final steady stress is not determined by the applied shear rate. To create the bands, a translational symmetry must be broken, but (unlike the pipe) each streamline is in principle equivalent. The symmetry must be broken by fluctuations, implying that the pattern of the bands (i.e. how many bands there are, and what thickness they have) is not determined by the shear rate, but rather by thermal fluctuations or other perturbations. In the next section, we will discuss these issues at the level of linear perturbations on a homogeneous flow.

4. Linear Analysis

In this section, we ask whether linear stability analysis provides any insights into band formation, with shear rate as the control parameter. The question of linear stability of uniform shear flow was considered by Yerushalmi *et al.* [4]. Here we are interested in the subsequent evolution of an unstable shear flow. In particular, we would like to discover the volume fractions of the two types of band, x_A and x_B, which is equivalent to knowing the stress S. It is possible that certain wavelengths of an initial perturbation grow preferentially in the linear regime, and that this is how bands begin to form. We will take the constitutive law to be completely general, and the fluid density ρ to be small, but non-zero.

Consider a uniform shear flow, with a steady shear rate of $\kappa = U/L$, producing a viscoelastic shear stress $\sigma^{ss}(\kappa)$, where 'ss' stands for 'steady shear'. The fluid velocity v is given by

$$v(y) = \kappa y \tag{13}$$

whilst the total stress, independent of position, is $\sigma^{ss}(\kappa)+\eta\kappa$. Now consider (1+1)-dimensional perturbations $\Delta\sigma(y,t)$ and $\Delta v(y,t)$. Linearise the constitutive equation around steady shear rate κ and write it as

$$\Delta\sigma(t) = G\int_0^\infty \mathrm{d}t' K(t'/\tau;\kappa)\frac{\partial\Delta v(y,t-t')}{\partial y}, \tag{14}$$

where G is the characteristic modulus of the material, and τ is its (terminal) relaxation time. The memory kernel K must depend on the shear rate κ. Note that $\mathrm{d}\sigma^{ss}(\kappa)/\mathrm{d}\kappa = G\int_0^\infty K(t/\tau)\mathrm{d}t$. Using equation (5) to eliminate the stress leaves this equation for Δv:

$$\rho\frac{\partial\Delta v}{\partial t} = \eta\frac{\partial^2\Delta v}{\partial y^2} + \frac{\partial}{\partial y}G\int_0^\infty \mathrm{d}t' K(t'/\tau;\kappa)\frac{\partial\Delta v(y,t-t')}{\partial y} \tag{15}$$

Write Δv as a Fourier series:

$$\Delta v(y,t) = \sum_{n=1}^{\infty} v_n(t)\sin\left(\frac{n\pi y}{L}\right). \tag{16}$$

Here we have assumed non-slip boundary conditions, $\Delta v(0) = \Delta v(L) = 0$, but the calculation could be done with any other linear boundary condition, and the final conclusion would be the same. In terms of the Fourier components, equation (15) becomes

$$\rho\frac{\partial v_n}{\partial t} = -\eta\left(\frac{n\pi}{L}\right)^2 v_n(t) - \left(\frac{n\pi}{L}\right)^2 G\int_0^t \mathrm{d}t' K((t-t')/\tau;\kappa)v_n(y,t'). \tag{17}$$

Taking v_{n0} to be the initial ($t=0$) value of $v_n(t)$, and Laplace transforming in t:

$$sv_n(s) - v_{n0} = -\frac{\eta}{\rho}\left(\frac{n\pi}{L}\right)^2 v_n(s) - \frac{G\tau}{\rho}\left(\frac{n\pi}{L}\right)^2 K(s\tau;\kappa)v_n(s) \tag{18}$$

Now, the problem contains three dimensionless parameters, the Weissenberg number $\mathrm{We} = \kappa\tau$, the Reynolds number $\mathrm{Re} = \rho LU/G\tau$, and the ratio of viscosities $\eta^* = \eta/G\tau$. It is useful to define $\rho_n^* = \mathrm{Re/We}(n\pi)^2 = (\rho/G\tau^2)(L/n\pi)^2$, which measures the inertia of the nth mode relative to the viscoelastic forces. After a rearrangement,

$$v_n(s) = \frac{\rho_n^* v_{n0}\tau}{s\tau\rho_n^* + \eta^* + K(s\tau;\kappa)}. \tag{19}$$

The perturbation is unstable if $s\tau\rho_n^* + \eta^* + K(s\tau;\kappa)$ has a zero in the right-hand half of the complex plane, for any value of n. The formalism above is equivalent to that of reference [4], where it was shown that a sufficient condition for instability is that $\eta^* + K(s=0) < 0$, i.e. that $(\mathrm{d}/\mathrm{d}\kappa)(\sigma^{ss}(\kappa) + \eta\kappa) < 0$ — the steady shear stress is a decreasing function of the shear rate. Here, we need to know, given the presence of an instability, which wavelengths of the perturbation grow most rapidly. The growth rate of any given Fourier component is the real part of the position on the complex plane of the rightmost zero of $s\tau\rho_n^* + \eta^* + K(s\tau;\kappa)$, and we must find out how this varies as a function of n. Assume that $K(t/\tau)$ can be written as the sum of a finite number of exponentials

$$K(t/\tau) = \sum_{q=1}^{Q} K_q\exp(-c_q t/\tau) \tag{20}$$

so that

$$K(s\tau) = \sum_{q=1}^{Q} \frac{K_q}{s\tau + c_q} \tag{21}$$

This is not a serious restriction. Differential constitutive equations are likely to satisfy it naturally. For example, the corotational Maxwell model has only two variables in the present flow geometry, the shear stress and the first normal stress difference, so (after linearising) the relaxation spectrum can have only two decay rates. By contrast, an integral equation, like the Doi-Edwards equation, has, in effect, an infinite number of variables, because to define the state of the system at any given time, we must specify an entire probability distribution (that of tube segment orientations). This implies an infinite number of relaxation times. However, it is possible to reduce the distribution function to a finite number of variables (e.g. by discretising it, or by expanding it in basis functions to finite order), and this should not change the qualitative behaviour; such a change would be unphysical. We infer that, to an arbitrary degree of accuracy, the relaxation spectrum can be replaced by a finite number of discrete relaxation times.

We are thus interested in the roots of the equation

$$s\tau\rho_n^* + \eta^* + \sum_{q=1}^{Q} \frac{K_q}{s\tau + c_q} = 0. \tag{22}$$

The ρ_n^* are extremely small. For example, the density of water is $\rho = 10^3$ kg m^{-3}, and for the cetylpyridinium system studied in reference [11], the modulus G and relaxation time τ are of order 30 Pa and 10 s respectively. The separation of the plates L may be 5×10^{-4} m. Therefore, $\rho_n^* = (\rho/G\tau^2)(L/n\pi)^2 = 10^{-8}/n^2$, and it is enough to consider the limit $\rho_n^* \to 0$. Rearranging,

$$\rho_n^*(s\tau)^{Q+1} + \rho_n^*(s\tau)^Q \sum_{q=1}^{Q} c_q + \eta^*(s\tau)^Q + \sum_{p=0}^{Q-1} (s\tau)^p \{\rho_n^* a_p + \eta^* b_p + f_p\} = 0 \tag{23}$$

where the a_p and b_p are functions of the c_q and the f_p are functions of the c_q and K_q. This is a singular perturbation problem. In the limit $\rho_n^* \to 0$, there is one singular root $s^{\text{sing}}\tau = -\eta^*/\rho_n^*$ and Q further roots which do not depend on ρ_n^*. s^{sing} is necessarily negative, and therefore corresponds to a decaying solution. None of the other roots depends on n. We conclude that, when a uniform shear flow is unstable, perturbations of that uniform flow grow at the same rate, irrespective of length-scale, as long they remain in a linear regime. If a banded flow emerges, this implies that it must have structure at all length-scales, or in other words, that there are bands of indefinitely narrow width. This is presumably unphysical. There are three alternatives: either a characteristic band width emerges only after the perturbations have already become large; or the 1-dimensional model here is inadequate, and the essential phenomena take place in 2 (or 3) dimensions; or the underlying constitutive model is deficient, and must be modified so as to intrinsically define a characteristic length-scale. These hypotheses are discussed in Sections 5, 6, and 7 respectively.

5. Numerical Analysis of the (1+1)-Dimensional Model

In this section, we will calculate the flow without making the assumption that it is nearly uniform. This must be done numerically, so we will use the toy constitutive equation (6).

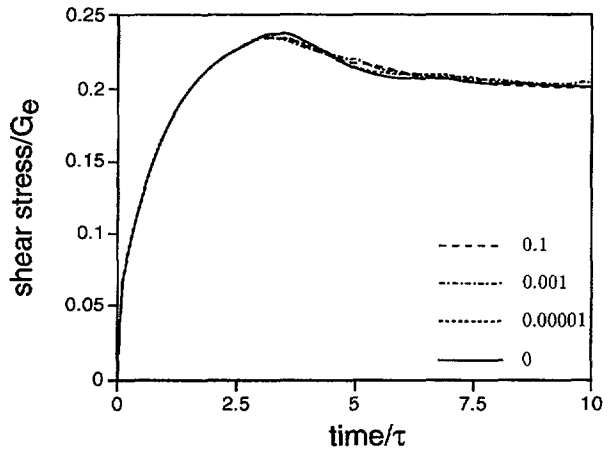

Fig. 3. — The start-up of steady shear flow, using the toy constitutive model, equations (6), (7), and different values of the fluid density.

Figure 3 shows solutions of equation (5) — the stress felt by the plates, as a function of time, after start-up of steady shear flow — with several values of ρ. We take $G = \tau = L = 1$ (without loss of generality), the shear rate $\kappa = U/L = 5$ (well inside the regime of decreasing stress), and the Newtonian solvent viscosity $\eta = 0.01$. In the cetylpyridinium system, ρ has a dimensionless value of the order of 10^{-7} Here we use some larger values, and also the case of creeping flow, $\rho = 0$.

Velocity and stress are defined on separate grids (offset by one half lattice spacing), and the parabolic equation (5) is solved by a fully-implicit method. The lattice spacings are $\Delta y = 0.02$ and $\Delta t = 0.01$. The initial condition is $v = \kappa y$ everywhere (this is only relevant for nonzero ρ), while σ, at each value of y, is initially an independent Gaussian random variable, with mean 0 and standard deviation 10^{-5} (if the initial condition does not contain some noise, the simulation is liable to predict a homogeneous shear flow, which we know to be physically unstable). For creeping flow, there is no need to solve a partial differential equation. Equation (12) is used in place of (5).

As can be seen from Figure 3, the results are virtually independent of the presence or absence of a small inertial term. Notice the overshoot. This arises directly from the development of a banded flow, because the toy equation can only ever describe monotonic (exponential) relaxation onto the steady state.

The viscoelastic part of the stress is shown as a function of both position and time in Figures 4 ($\rho = 0.001$) and 5 ($\rho = 0$). This is related to the local shear rate by equation (12), so a larger viscoelastic stress corresponds to a lower shear rate. In both figures, by time 2, the fluctuations have started to become significant (of course, in the linear regime, their actual size is proportional to the initial values), and by time 5, two distinct phases have developed. At time 10, the relaxation toward the steady state has begun, and by time 20, it has essentially been reached. The presence of a small amount of inertia makes no difference; in any case, the bands have a thickness of the order of the numerical grid spacing.

This apparently unphysical result is not a failing of the numerical technique, but seems to be inherent in the model. Equation (5) is a diffusion equation, with diffusion coefficient η/ρ. When ρ is very small, the time taken to diffuse across the space between the plates becomes arbitrarily small. Therefore, each streamline is as strongly coupled to distant streamlines as it

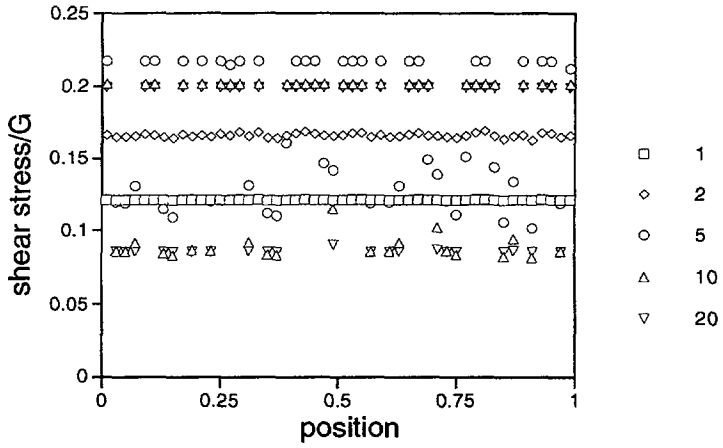

Fig. 4. — The viscoelastic stress as a function of position, at several times after the onset of steady shear. The fluid density is 0.001. The horizontal axis extends from the first plate (position 0) to the second plate (position 1).

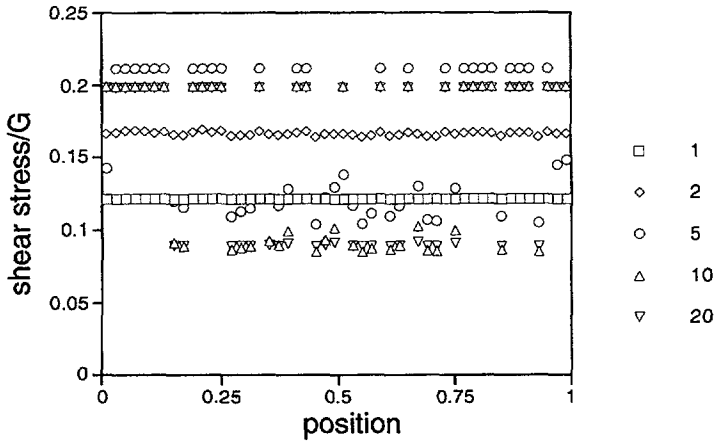

Fig. 5. — As Figure 4, but with no inertia.

is to its neighbours. ($\sigma(y)$ can change only on the time-scale of the viscoelastic relaxation time, so, on the diffusive time-scale, it is effectively fixed.) This is why equation (12) gives $\partial v/\partial y$ in terms of the average σ. It also implies that macroscopic bands cannot be produced, because that would require neighbouring streamlines to be correlated, when in fact each streamline — each value of y — is a separate dynamical system, coupled to the others only *via* equation (12). Of course, the same result was obtained in the previous section by linear analysis, where it was found that there was no preferred length scale for bands. The numerical calculations have an extra length scale, the grid spacing, and select this as the band width.

It appears that it is not possible to obtain a realistic flow pattern even when the full nonlinear dynamics are accounted for, at the (1+1)-dimensional level of analysis. Leaving aside this difficulty for the moment, we will ask what behaviour the model does have. An important

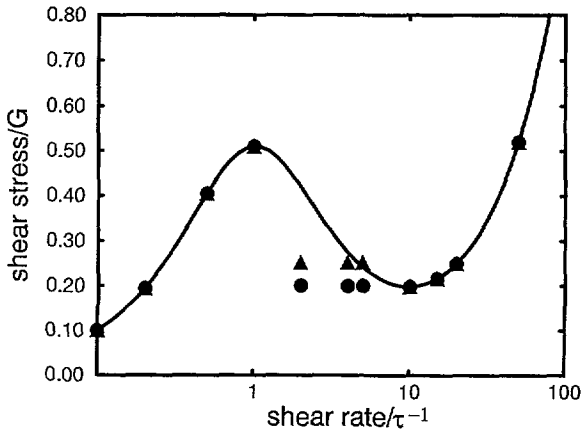

Fig. 6. — The final steady shear stress in the simulated banded flow (using the toy constitutive equation) (points). The circles are for the unmodified toy equation, equation (6), and the triangles for the model with a stress diffusion constant, equation (26). The solid line is the steady stress assuming homogeneous flow. The Newtonian viscosity η is 0.01 in each case.

question is the final steady stress in the material after the banded flow has developed. The final stress from band simulations is shown in Figure 6 (for a range of shear rates, with $\rho = 0$, and other parameter values and initial conditions as for Fig. 3).

Similar calculations have been done by Español *et al.* for a different constitutive model (that of Johnson and Segalman, with a single relaxation time), with a very similar result [26]. Clearly, the stress associated with banding is near the minimum in the underlying constitutive curve, whereas, in [10], the assumption was made that the stress would be near the *maximum* of the curve. These simulations were done by starting from zero stress, and applying a constant shear rate. It may be that the final stress is dependent on the previous shear-rate history, so that a maximum-stress banded state, as postulated in [10], could be created by using an appropriate sequence of shear rates. It is plausible that this can be done by slowly increasing the shear rate from zero. This would mean that, by the time the unstable shear-rate regime is entered, the material is already in a state in which the stress has the desired value. This also simulates viscometric experiments in which the shear rate is slowly increased, with a measurement being made at each shear rate.

To test this idea, we show in Figure 7 the effect of a slowly increasing shear rate on the toy equation, without inertia. Shortly after the critical shear rate is passed, the stress drops dramatically as a banded flow develops near the *minimum* stress. As the shear rate is further increased, the band-structure remains invariant — the proportion of each type of band remains the same, but the shear rates and stresses increase. Eventually the maximum stress is reached again, the stress drops, and a new band-structure is created with a higher proportion of the high-shear phase. This happens several times. A similar result is obtained if the fluid is given some inertia by setting $\rho = 0.001$.

This behaviour can be understood as follows. It is easier to make a small change in the shear rate and stress of a whole band, than it is to change the size of the band. To do that requires the boundary between bands to be moved, so that the material on the boundary has to be subjected to a different shear rate (for a period of several relaxation times) to bring it into a new steady state. McLeish and Ball argued that this cannot be achieved by a small

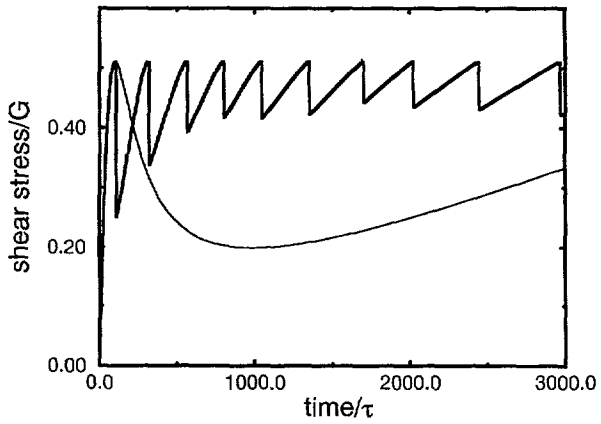

Fig. 7. — The shear stress, using the toy equation, as a function of time (heavy line). The shear rate is increased smoothly from 0 at time 0, at $0.01\tau^{-2}$. The thin line shows the steady stress for homogeneous flow, at the same shear rate. $\Delta y = 0.001$, $\Delta t = 0.01$, $\eta = 0.01$.

perturbation, because part of the material would change its stress by a finite (as opposed to infinitesimal) amount [7]. Instead, the stress changes throughout the material. When the low shear-rate phase has reached the maximum stress, it becomes unstable against fluctuations, which therefore grow until parts of the low shear bands have changed into the high-shear phase. As the shear rate is increased, this happens several times, giving rise to the sawtooth pattern. A 'cure' for this physically implausible behaviour is proposed in Section 7.

5.1. The Micelle Reptation-Breaking Equation. — An integral constitutive equation should be tested, to see whether it behaves in the same way as the differential models considered above. Since shear-banding has been claimed for a wormlike micelle system, we will use the constitutive equation proposed for these materials.

Entangled polymers are described using the tube model, in which each chain is assumed to be confined to a tube by the surrounding molecules. Doi and Edwards devised a constitutive equation using this idea [1]. Wormlike micelles can entangle in the same way as polymers, the most important difference being that they can break and reform reversibly. Cates adapted the model of Doi and Edwards to include the effect of these breaking reactions [13,27]. The resulting constitutive equation is very similar to that of Doi and Edwards, and a brief description of it is given in the Appendix.

We have done simulations of banded flow, similar to those with the toy equation, in which we solve the micelle reptation-breaking model using the stochastic method of Öttinger [28] (see Appendix).

5.2. Band Simulations Using the Micelle Equation. — Figure 8 shows the startup of shear flow (from equilibrium) with the micelle equation and a range of shear rates (without inertia). A Newtonian viscosity of 0.001 is now used, since the viscoelastic stress falls away more slowly at high shear rate than for the toy model, equation (6). Bands are present at the higher shear rates. The distribution of the viscoelastic stress (i.e. the band structure) is similar to that of Figures 4, 5, but rather noisy because of the stochastic algorithm. The final steady stress is shown in Figure 9.

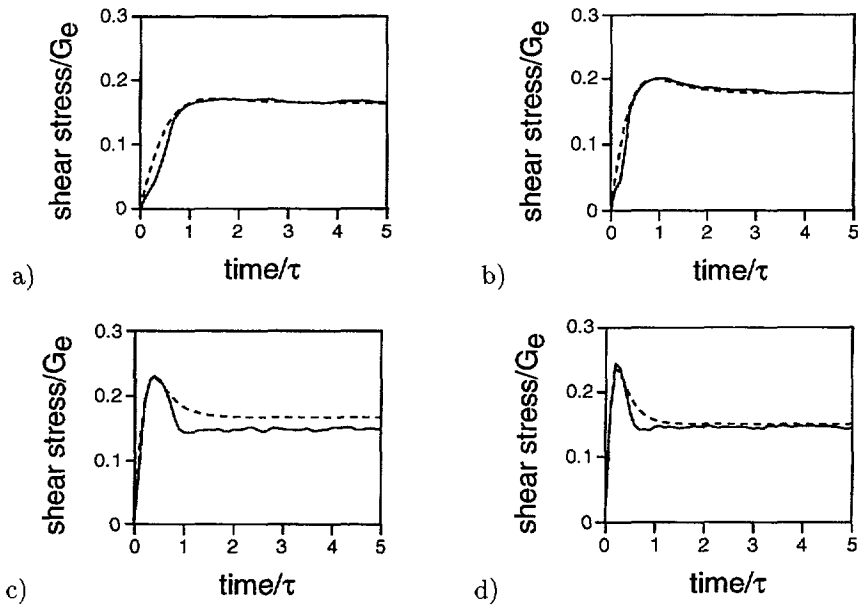

Fig. 8. — Start-up of shear flow for the micelle equation at (a) $1.275\tau^{-1}$, (b) $2.125\tau^{-1}$, (c) $5.1\tau^{-1}$ and (d) $8.5\tau^{-1}$ The solid lines show the simulated banded flow (solution of Eq. (12) coupled to the micelle reptation-breaking constitutive model), and the dotted lines show the solution of the same model assuming homogeneous flow

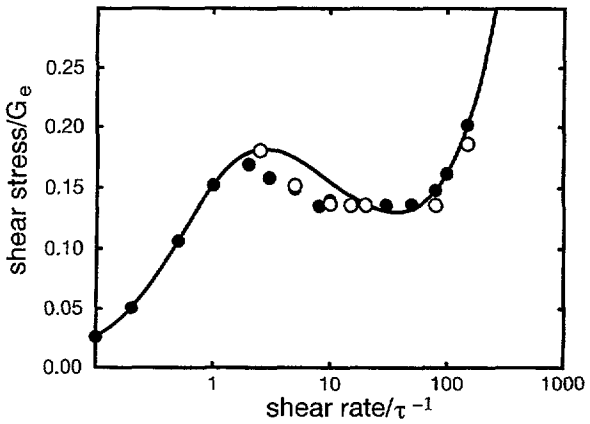

Fig. 9. — Final steady stress after start-up of steady shear flow, for the micelle model. The filled and open circles are for (1+1)- and 2-dimensional calculations respectively.

With the toy model, the formation of bands causes an overshoot in the shear stress, which could not be present otherwise. In contrast, the direct solution of the micelle constitutive equation for homogeneous shear flow (Fig. 8, dashed lines) already shows an overshoot, so we might expect this to be enhanced by the banding. In fact, this does not happen, and the overshoot is no larger than in the direct solution.

If we use a slowly increasing shear rate, a result similar to Figure 7 is obtained.

6. The 2-Dimensional Model

We have performed numerical calculations on the 2-dimensional model for micelles using a novel Lagrangian-Eulerian method. This uses a mesh which moves and deforms with the fluid, and has been used for shearing and extrusion flows [29,30]. It enables fairly high Weissenberg numbers to be reached, but, at present, is restricted to creeping flows (no inertia).

The method works as follows. The program stores the coordinates of some material points, about 300 in this work. The stress is defined at each of these points. At every time-step, the pressure and velocity fields are solved for, in Eulerian fashion. Then the positions of the points are updated by convecting them with the fluid flow. This is the Lagrangian part of the method. The velocity gradient at each point is also known, and used to update the stress. This procedure is repeated for each time-step, Figure 10.

To solve for the pressure and velocity, a grid must be laid over the material points. The Voronoi mesh is suitable, and it is defined as follows. Each material point is associated with one element of the mesh, and that element contains all of the space closer to that material point than to any other. Thus, the material point is at the centre of an element, and, for the purpose of finding the pressure, is deemed to be connected to the material points associated with all of the neighbouring elements. If any element of the grid becomes too distorted as the material points move, the Voronoi mesh is reconnected. More details are given in reference [29].

The pressure and velocity must be found subject to the boundary conditions, the requirement of incompressible flow, $\nabla \cdot \mathbf{v} = 0$, and the creeping flow condition, $\nabla \cdot (\boldsymbol{\sigma}^{\text{visco}} + \boldsymbol{\sigma}^{\text{Newt}}) - \nabla p = 0$. $\boldsymbol{\sigma}^{\text{visco}}$ is the viscoelastic contribution to the stress, and $\boldsymbol{\sigma}^{\text{Newt}} = \eta(\nabla \mathbf{v} + \nabla \mathbf{v}^{\text{T}})$ is the Newtonian. The solution is found by iterating

$$\mathbf{v}^{n+1} = \mathbf{v}^{n} + \beta_1 \left(\nabla \cdot (\boldsymbol{\sigma}^{\text{visco}} + \boldsymbol{\sigma}^{\text{Newt}}) - \nabla p \right) \tag{24}$$

$$p^{n+1} = p^{n} + \beta_2 \left(\nabla \cdot \mathbf{v} \right) \tag{25}$$

until the solutions have converged to within the required tolerance. β_1 and β_2 are relaxation parameters.

To calculate the stress, a constitutive relation is required. Both differential and integral equations have been used in previous work [29]. Here we use the micelle reptation-breaking model described above, and solve it using the stochastic method. For each material point, 1000 vectors are stored, and updated every time-step. Ours is the first work to combine the Voronoi finite element procedure with this efficient method [28] of implementing an integral constitutive equation.

Our calculation was a simulation of planar Couette flow. The plate separation was L, with boundary conditions specified by equations (3)–(4). The simulation space extended distance $L/2$ in the longitudinal (x-) direction, with periodic boundary conditions. The time-step used was 0.01 (with the viscoelastic relaxation time taken as the unit of time), and the Newtonian solvent had viscosity 0.001. The initial condition was equilibrium, and a constant shear rate was instantaneously switched on.

6.1. RESULTS. — The final steady state was a banded flow for shear rates in the unstable, decreasing stress regime, as in the (1+1)-dimensional problem. A typical band profile is given in Figure 11. This shows the local shear rate as a function of the transverse coordinate y, in the steady state. The points are averages over time and the longitudinal coordinate x. The errors arise from the numerical noise. Notice that the band is broad and macroscopic, unlike the (1+1)-dimensional calculation. The position of the band is random, but its width (or, equivalently, the shear stress) appears to be determined by the shear rate. The edges of

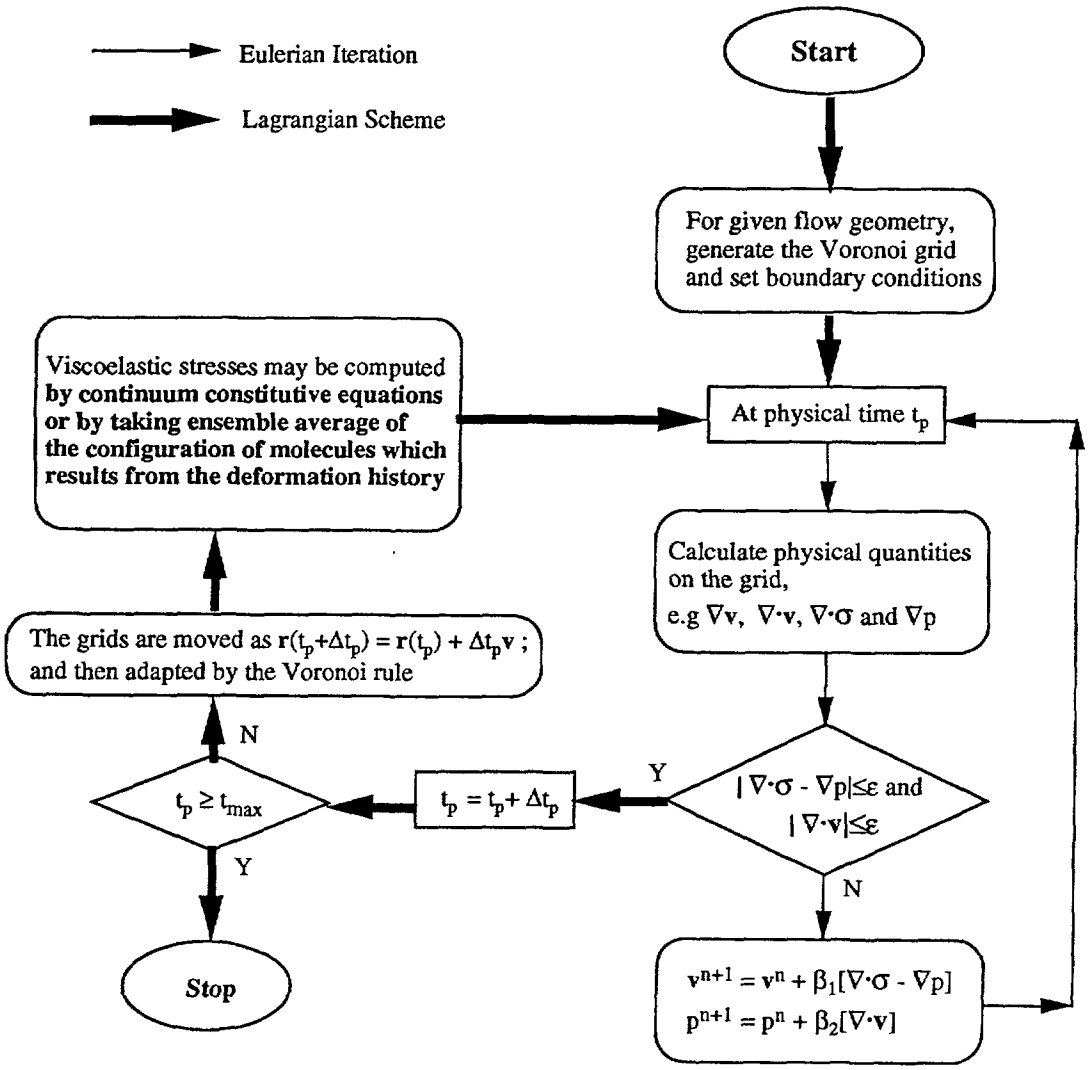

Fig. 10. — Flowchart for the Lagrangian-Eulerian method used for the two-dimensional calculations.

the band are blurred, and because of the noise, it is unclear whether this is due to physical undulations in the interface (implying a somewhat unsteady flow) or to numerical effects. The final shear stress is shown in Figure 9, and this is almost unchanged from the (1+1)-dimensional case.

Our calculations in the 2-dimensional model have given a more realistic band pattern than the (1+1)-dimensional. The final steady stress, as a function of shear rate, is not much changed. We note that equivalent calculations have been carried out by Español *et al.* for the Johnson-Segalman fluid [26], with results similar to those here.

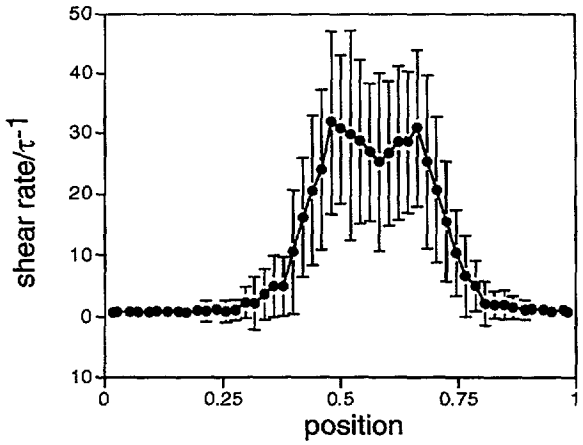

Fig. 11. — Band pattern arising from a 2-dimensional calculation of start-up of steady shear at $10\tau^{-1}$. The local shear rate in the steady state is given as a function of lateral coordinate y. The points are an average in time and along the shear flow (x-) direction, and the bars are the corresponding standard deviation.

7. Interface Effects

We now focus our attention on the interface between shear bands. We expect that, like every other interface found in nature, this must have some non-zero (though possibly quite small) width. Our discussion is motivated by our calculations with the (1+1)-dimensional model, in which we found structure at indefinitely short length-scales. Presumably, this structure is cut off at some microscopic length, which would then be the interface width.

To take account of these effects requires the constitutive model to be altered. Again consider the toy model, equation (6), and now suppose that interfacial effects have an energy cost of $E_{\text{interface}} \propto \int_0^L \mathrm{d}y(\partial\sigma/\partial y)^2$. Recall that σ is the viscoelastic contribution to the total stress. It is an average over the microscopic configuration of the viscoelastic material and therefore has something of the character of an order parameter. Expansions of the free energy in powers of an order parameter usually include a gradient-squared term [31], and it is just this term that we use as our expression for $E_{\text{interface}}$.

Now include in equation (6) a term of the form $\gamma\partial E_{\text{interface}}/\partial\sigma$, giving

$$\frac{\partial\sigma}{\partial t} - \gamma\frac{\partial^2\sigma}{\partial y^2} + \frac{\sigma}{\tau} = Gg\left(\tau\frac{\partial v}{\partial y}\right). \tag{26}$$

This is similar to the usual approach to linear non-equilibrium thermodynamics, which is not rigorously justified here, because the system is far removed from equilibrium. Our derivation should therefore be regarded as phenomenological. (Ref. [32] obtains a similar result from a microscopic model.) Notice that γ has the dimensions of a diffusion coefficient, so the interface will have thickness of order $(\gamma\tau)^{1/2}$. Equation (26) has already been studied by Brunovský and Ševčovič in the context of slit channel flow [33].

As in Section 3, we may eliminate $\partial v/\partial y$ and replace the 'force' g with the 'potential' V. With the new term, equation (9) becomes

$$\frac{\partial\sigma}{\partial t} - \gamma\frac{\partial^2\sigma}{\partial y^2} = -\frac{1}{\tau}\frac{\partial V(\sigma)}{\partial\sigma} \tag{27}$$

In the steady state, $\partial\sigma/\partial t = 0$, and we have

$$\gamma\tau\frac{\partial^2\sigma}{\partial y^2} = \frac{\partial V}{\partial\sigma} \tag{28}$$

σ is therefore equivalent to the position of a particle moving in a potential $-V$ (with y as the time variable and $\gamma\tau$ as the mass). Assume that we have controlled stress, and that $S_{\min} < S < S_{\max}$. Therefore, $-V$ has two maxima.

Now, a banded flow has σ constant through the first band, followed by a rapid transition as we pass through the interface, followed by a different constant in the second band. This corresponds to the particle sitting on top of one of the maxima (for an extended period of time), then rolling down through the minimum, coming to rest on top of the other maximum, and remaining there. Of course, because of energy conservation, this is only possible if the maxima have the same height, and this will only be true for one particular applied stress. We deduce that only for this one stress can shear bands coexist. For the toy model, with potential V given by equation (10) and $G = \tau = 1$ and $\eta = 0.01$, this value is $S = 0.251$. This is in contrast to the case without the interfacial term, discussed in Section 3, where a banded flow could exist, at least in principle, for any stress between $S_{\min}$ and $S_{\max}$. Of course, what we have shown in each case is that a banded flow is a stationary solution of the equations of motion for our model system. To actually create a banded flow in the controlled-stress regime, as already discussed in Section 3, would require careful and deliberate manipulation of the stress, and might even be impossible in practice.

What if the stress does not have the coexistence value? Postulate a time-varying solution of the form $\sigma = f(y - ut)$. This gives us

$$\gamma\frac{\partial^2 f}{\partial y^2} + u\tau\frac{\partial f}{\partial y} - \frac{\partial V(f)}{\partial f} = 0. \tag{29}$$

This equation describes our particle, moving in the same potential, but with a friction constant $u\tau$. The particle can now begin on the higher of the two maxima, travel through the valley and come to rest on the other maximum, exactly as before, even though the maxima have different heights. The surplus energy is dissipated during the journey. This means that the function f has the same qualitative form as the stress profile in the coexistence case, albeit now with non-zero u. Thus, a transient band structure is possible. The interface travels at a speed u, determined by the height difference between the maxima, and therefore by the applied stress. Eventually, the interface will reach one of the rheometer plates and disappear, leaving a homogeneous flow as the final steady state.

Olmsted and Goldbart studied similar phenomena in the context of the shear-induced isotropic-to-nematic transition [34]. Their equations included surface energy terms which arise naturally from the model of a nematogen used, but are similar in essence to the one here. They studied the propagation of the interface between two non-equilibrium phases, and located the coexistence point by finding the stress for which the interface no longer moves. A similar technique has been used for the driven diffusive lattice gas by Krug *et al.* [35].

With shear rate as the control parameter, we anticipate that the interface moves in the same way. Now the stress adjusts, according to $S = \langle\sigma\rangle + \eta\kappa$, as the proportion of each type of band changes. The final steady state would then be a banded flow at the coexistence stress.

The results of simulated start-up experiments (in (1+1)-dimensions) are shown in Figure 6. The density $\rho = 0$ (creeping flow), the stress diffusion constant γ is 10^{-4}, the numerical grid size $\Delta y = 0.001$, and other parameters have the same values as previously. As expected, in the decreasing stress regime, the coexistence stress, $S = 0.25$, is selected. (Recall that this is the

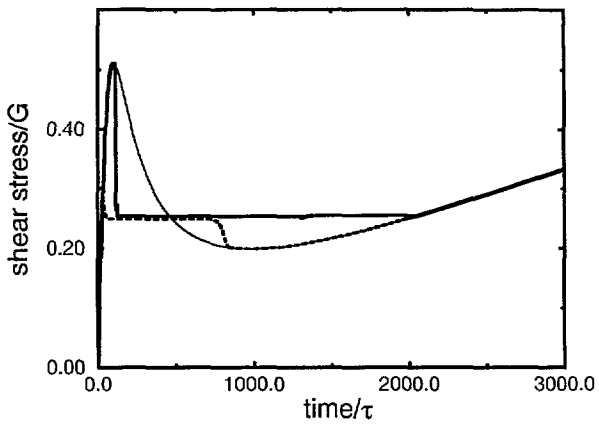

Fig. 12. — The heavy line shows the effect of a steadily increasing shear rate, as for Figure 7, on the toy constitutive model with a diffusion term (Eq. (26)). The thin line is the stress corresponding to homogeneous flow at the same shear rate. The dotted line corresponds to a decreasing shear rate, starting at $30\tau^{-1}$ at the right hand side and reaching zero at the left.

value of S for which $V(\sigma_A) = V(\sigma_B)$, where σ_A and σ_B are the viscoelastic stresses in the low and high shear rate bands respectively.) The corresponding flow pattern (not shown) contains one or two broad bands at each shear rate.

If the shear rate is swept continuously, the stress behaves as in Figure 12 (heavy line). The corresponding calculation without the diffusive (interfacial energy) term is given in Figure 7. In each case, when the shear rate is increased past the threshold of instability κ_1, a banded flow develops. However, with the new model, the stress remains constant as the shear rate is further increased. The proportion of the two types of band is changing, which is possible because the modified model allows the interface between them to move. Eventually, all of the low-shear material is eliminated, and a uniform flow is recovered at the high shear-rate branch. The dashed line shows the effect of decreasing the shear rate (so the time axis now reads from 0 at the right hand side to 3000 at the left). Hysteresis is observed; the uniform flow persists until the upper stability threshold κ_2 is met.

The behaviour in Figure 12 seems to be much more realistic than that in Figure 7, although it does not quite reproduce the experimental rheological measurements of references [11, 15]. The experiments show a stress which initially increases with shear rate and then goes smoothly into a plateau, whilst the birefringence of the low-shear phase shows a kink but is continuous (in the mathematical sense). Thus, the stress and optical properties of the homogeneous phase immediately prior to band formation are the same as those of the low-shear band immediately after. This is in contrast to the behaviour shown in Figure 12, where the stress immediately before is S_{max} (as defined in Fig. 1) and the stress afterwards is the coexistence stress. This suggests two possible explanations. Firstly, the bands could be forming as soon as the coexistence stress is reached, even though the system is not yet mechanically unstable, by nucleation of a high shear-rate band. (For a discussion of nucleation in the context of shear-induced nematic phases, see Ref. [17]). Alternatively, the coexistence stress might happen to be very close to the stress at which the mechanical instability occurs (i.e. S_{max}), so that the stress overshoot in Figure 12 is present but too small to detect.

We have not attempted to calculate the properties of a two-dimensional model with the new interfacial term. However, it is clear that this term will create a surface tension in the interface

between bands, which will suppress fluctuations in the interface, and therefore presumably tend to increase the stability of the banded flow.

8. Conclusions

We have shown that a nonmonotonic constitutive relation produces a banded flow in steady shear at the (1+1)-dimensional level of analysis. However, the bands have indefinitely narrow width. Numerical calculations in two dimensions produce broad bands, but it not yet clear whether this is a real steady-state property of the 2-dimensional model, or simply an artefact of the numerical algorithm. The final steady shear stress after start-up of shearing at a given rate is unaltered from the (1+1)-dimensional problem, which may be an indication that no new physics is involved.

Even at the (1+1)-dimensional level, the unphysical narrow bands are avoided if a term is added into the constitutive model to allow for the inhomogeneity in the material. Even if the coefficient associated with this term is very small, the behaviour of the system is qualitatively changed. The modification produces broad, macroscopic bands, and the final stress after start-up is also different. The new constitutive model allows the position of the interface between bands to move, and the stress is therefore selected by a coexistence criterion between the two phases (low and high shear rate). Although we have considered only systems in states far removed from equilibrium, there is a close analogy with equilibrium phase coexistence.

Acknowledgments

We are grateful to G. Marrucci, T. C. B. McLeish, F. Greco, R. C. Ball, P. Español, P. D. Olmsted and D. Drasdo for interesting discussions. N. A. S. acknowledges the financial support of the EPSRC and Shell Research (in the form of a CASE award) and of the Max Planck Gesellschaft. The work of X. F. Y. has been funded by the DTI Link project and by a grant from the BBSRC. This research was funded in part by the EC Network contract ERBCHR XCT 94 04 86.

Appendix A

Here we give a short description of the reptation-breaking model for wormlike micelles and its stochastic implementation. For details, see references [13,27,28].

The micelle is contained inside a tube, which we imagine to be divided into segments. Now, every time a breaking or recombination reaction takes place, the length of the micelle changes. Therefore, a segment does not have a well-defined position within the tube. Every segment has belonged to chains of a whole range of lengths, and been at a range of different positions within those chains. Every segment is statistically equivalent, and we need not distinguish segments by position in the tube. This is in contrast to unbreakable polymers, where every tube position has a different distribution of segment orientations.

The micelle moves along the contour of the tube in a one-dimensional curvilinear Brownian motion ('reptation'). The breaking reactions couple to reptation in such a way that tube segments are supposed to be continually destroyed at a rate $\mathcal{D}$, and new ones created to replace them at rate $\mathcal{B}$. The new segments have random orientations with an isotropic distribution. The stress is related to the segment orientations $\mathbf{u}$ by

$$\boldsymbol{\sigma} = G_e \langle \mathbf{uu} \rangle \tag{A.1}$$

where the average $\langle \cdots \rangle$ is taken over every segment in the material. In the presence of a flow, each tube segment is deformed affinely. The following constitutive equation results:

$$\boldsymbol{\sigma}(t) = G_e \int_{-\infty}^{t} \mathcal{B}(t') \exp\left[-\int_{t'}^{t} dt'' \mathcal{D}(t'')\right] \tilde{\mathbf{Q}}(\mathbf{E}_{t't})\, dt'. \tag{A.2}$$

This is an integral over all past times t'. The integrand is the contribution to the stress from segments created at t'. This contribution is equal to the stress per segment, $\tilde{\mathbf{Q}}$, multiplied by the number of segments created at t', $\mathcal{B}(t')$, multiplied by the probability that a segment survives from t' to t (the exponential). Also, $G_e = 3(c/N_e)k_BT$, where c is the concentration of monomers, and N_e is the degree of polymerisation per entanglement (so c/N_e is the number of entanglements per unit volume). $\mathbf{E}_{t't}$ is the deformation tensor from time t' to time t. $\tilde{\mathbf{Q}}$ is given in terms of it, by

$$\tilde{\mathbf{Q}}(\mathbf{E}_{t't}) = \left\langle \frac{(\mathbf{E}_{t't}.\mathbf{u})(\mathbf{E}_{t't}.\mathbf{u})}{|\mathbf{E}_{t't}.\mathbf{u}|} \right\rangle_0 \tag{A.3}$$

where the average is taken over the isotropic distribution.

$\mathcal{B}$ and $\mathcal{D}$ have yet to be found. In the absence of a flow, they are both equal to $1/\tau$, where τ is the viscoelastic relaxation time. In the presence of a flow, this is no longer true. In particular, the affine deformation of the segments tends to increase the total tube length, so $\mathcal{D}$ increases to compensate. Assuming, as an approximation, that $\mathcal{B}$ is unchanged, we have

$$\mathcal{B} = \frac{1}{\tau} \tag{A.4}$$

$$\mathcal{D} = \frac{1}{\tau} + (\nabla \mathbf{v})^{\mathrm{T}} \cdot \langle \mathbf{uu} \rangle \tag{A.5}$$

where $\mathbf{u}$ is the orientation of a tube segment, and the average $\langle \cdots \rangle$ is taken over all segments in the material.

Following Öttinger [28], this model may be solved stochastically. We maintain an ensemble of N vectors, each of which represents one tube segment. The total length of the vectors is arbitrary, so we take it to be unity. On each time-step, every vector is deformed affinely, according to this equation

$$\mathbf{r} \leftarrow \mathbf{r} + \Delta t (\nabla \mathbf{v})^{\mathrm{T}} \cdot \mathbf{r}. \tag{A.6}$$

A fraction $\Delta t/\tau$ of the vectors are eliminated, and replaced by new vectors with random orientation and length $1/N$; this simulates the reptation-breaking relaxation process occurring at rate $1/\tau$. All the remaining vectors are then scaled by a constant factor, chosen so as to restore the total length to 1, and this takes account of the enhanced segment destruction rate in the presence of a flow. This procedure gives the same results as the model described above. The stress tensor is given by

$$\boldsymbol{\sigma} = G_e \sum \mathbf{rr} \tag{A.7}$$

where the sum is taken over all the vectors in the ensemble. A separate ensemble is required for every numerical grid element in a simulation. For all the calculations presented here, N was 1000 vectors per element.

References

[1] Doi M. and Edwards S.F., The Theory of Polymer Dynamics (Clarendon Press, Oxford, 1986).
[2] Larson R.G., Constitutive Equations for Polymer Melts and Solutions (Butterworth, Stoneham, 1988).
[3] Spenley N.A. and Cates M.E., *Macromolecules* **27** (1994) 3850.
[4] Yerushalmi J., Katz S. and Shinnar R., *Chem. Eng. Sci.* **25** (1970) 1891.
[5] Denn M.M., *Ann. Rev. Fluid Mech.* **22** (1990) 13.
[6] Larson R.G., *Rheol. Acta* **31** (1992) 213.
[7] McLeish T.C.B. and Ball R.C., *J. Polym. Sci. Part B–Polym. Phys.* **24** (1986) 1735.
[8] McLeish T.C.B., *J. Polym. Sci. Part B–Polym. Phys.* **25** (1987) 2253.
[9] Malkus D.S., Nohel J.A. and Plohr B.J., *J. Comp. Phys.* **87** (1990) 464.
[10] Cates M.E., McLeish T.C.B. and Marrucci G., *Europhys. Lett.* **21** (1993) 451.
[11] Rehage H. and Hoffmann H., *Mol. Phys.* **74** (1991) 933.
[12] Cates M.E. and Candau S.J., *J. Phys.: Condens. Matter* **2** (1990) 6869.
[13] Cates M.E., *J. Phys. Chem.* **94** (1990) 371.
[14] Spenley N.A., Cates M.E. and McLeish T.C.B., *Phys. Rev. Lett.* **71** (1993) 939.
[15] Makhloufi R., Decruppe J. P., Aït-ali A. and Cressely R., *Europhys. Lett.* **32** (1995) 253.
[16] Decruppe J.P., Cressely R., Makhloufi R. and Cappelaere E., *Colloid Polym. Sci.* **273** (1995) 346.
[17] Berret J.-F., Roux D.C. and Porte G., *J. Phys. II France* **4** (1994) 1261.
[18] Schmitt V., Lequeux F., Pousse A. and Roux D., *Langmuir* **10** (1994) 955.
[19] Berret J.-F., Roux D.C., Porte G. and Lindner P., *Europhys. Lett.* **25** (1994) 521.
[20] Cappelaere E., Cressely R., Makhloufi R. and Decruppe J.P., *Rheol. Acta* **33** (1994) 431.
[21] Malkus D.S., Nohel J.A. and Plohr B.J., *SIAM J. Appl. Math.* **51** (1991) 899.
[22] Nohel J.A. and Pego R.L., *SIAM J. Math. Anal.* **24** (1993) 911.
[23] Nohel J.A., Pego R.L. and Tzavaras A.E., *Proc. Roy. Soc. Edinburgh* **115A** (1990) 39.
[24] Johnson M.W. and Segalman D., *J. Non-Newt. Fluid Mech.* **2** (1977) 255.
[25] Schmitt V., Marques C.M. and Lequeux F., *Phys. Rev. E* **52** (1995) 4009.
[26] Español P., Yuan X.F. and Ball R.C., submitted to *J. Non-Newt. Fluid Mech.*
[27] Cates M.E., *Macromolecules* **20** (1987) 2289.
[28] Öttinger H.C., *J. Chem. Phys* **91** (1989) 6455.
[29] Yuan X.F., Ball R.C. and Edwards S.F., *J. Non-Newt. Fluid Mech.* **46** (1993) 331.
[30] Yuan X.F., Ball R.C. and Edwards S.F., *J. Non-Newt. Fluid Mech.* **54** (1994) 423.
[31] Rowlinson J.S. and Widom B., Molecular Theory of Capillarity (Clarendon Press, Oxford, 1989).
[32] El-Kareh A.W. and Leal G.L., *J. Non-Newt. Fluid Mech.* **33** (1989) 257.
[33] Brunovský P. and Ševčovič D., *Quart. Appl. Math.* **L2** (1994) 401.
[34] Olmsted P.D. and Goldbart P.M., *Phys. Rev.* **A46** (1992) 4966.
[35] Krug J., Lebowitz J.L., Spohn H. and Zhang M.Q., *J. Stat. Phys.* **44** (1986) 535.